DOI: 10.1002/ adom.201701154
Article type: Full Paper

Second harmonic generation manipulation enabled by electromagnetic coupling in bianisotropic metamolecules

*Kai Guo, Cheng Qian, Yong Liang Zhang, and Kin Hung Fung**

Dr. K. Guo
School of Computer and Information, Hefei University of Technology, Hefei, 230009, China

Dr. K. Guo, Dr. C. Qian, Dr. Y. L. Zhang, and Dr. K. H. Fung*
Department of Applied Physics, The Hong Kong Polytechnic University, Hong Kong, China

E-mail: khfung@polyu.edu.hk
Keywords: plasmonics, nonlinear optics, bianisotropy, metamolecule

Abstract: Bianisotropic metamolecules provide a novel opportunity to realize optical magnetism through localized electromagnetic coupling (EM coupling). Previous investigations of the EM coupling, however, are mostly limited to linear regime. In this work, we theoretically study active manipulation of light in nonlinear regime with EM coupling. To this end, we design a bianisotropic metamolecule composed of four uniform gold nanodisks. Simulation results show that a Fano-like resonance induced by EM coupling is sufficient to control second harmonic generation (SHG) signal. By rotating polarization angle of optical excitation source, we switch on-off of the emitted SHG signal with the EM coupling. Furthermore, we demonstrate modulation of the SHG signal through the EM coupling by tuning the gap size and filling material.

1. Introduction

When light propagates in medium or structures, its properties, including phase, polarization and frequency, could be controlled due to the light-matter interaction in different types of material such as anisotropy, birefringence, and nonlinearity. [1, 2] However, the ability of light-controlling in natural materials is restricted by the limited categories. Metamolecules or metamaterials stand out for their optical properties could be configurable by artificially

engineering the size, shape, materials and also the arrangement of the constituent.[3, 4] Over the past decades, a lot of fascinating optical properties have been achieved by using metamolecules or metamaterials, including unnatural refraction index,[5-11] hyperbolic anisotropy, [12-14] optical magnetism,[15-20] and nonlinearity. [21-27]

Among these novel phenomena, optical magnetism is of particular interest due to the weakness of magnetic response in optical materials. It has been recently both experimentally and theoretically demonstrated by tailoring metamolecule structures, such as metallic split-ring,[28-30] plasmonic nanoparticle clusters,[31-35] metal-insulator-metal oligomers,[36, 37] and plasmonic gratings.[38, 39] These artificial phenomena come from local electric-bright mode and magnetic-dark mode coupling (EM coupling) in nanostructures, which can be explained by using analytical theory approaches, [35, 40-44] and utilized to switch the electromagnetic responses.[45] In essence, most of these EM coupling effects come from bianisotropy, which has been of interest due to optical magnetism and its non-reciprocity. [38, 46, 47] Usually, EM coupling is accompanied by Fano-like features with near-field enhancement and far-field scattering suppression.[48] These capabilities are beneficial to both linear[49] and nonlinear[50-52] process down to a nanoscale volume.

In contrast to an extensive study on linear effect, EM coupling in bianisotropic nanostructure has been preliminarily investigated in nonlinear optical regime. Wen et al. proposed a pioneering mechanism for generating optical nonlinearity based on purely electromagnetic theory,[53] arising from magnetic-Lorentz-force (MLF),[54] which has been considered as a negligible component owing to low mobility of free electron and weak magnetic response of most natural material to electromagnetic wave. Yang et al. has exploited a plasmonic trimer to demonstrate that EM coupling resonance could have a chance to boost SHG effect in comparison with electric-multipolar resonances.[55] Nevertheless, we still suffer from poor knowledge of tuning/modulating interaction between optical nonlinearity and EM coupling at the nanoscale, which could introduce numerous new applications.

In this work, we numerically investigate the manipulation of SHG with EM coupling resonance in a bianisotropic metamolecule composed of four uniform gold nanodisks, focusing on both intensity and frequency of emitted SHG signal. First, in linear regime we reveal that a Fano-like resonance, coming from EM coupling, could be switched on and off by using orthogonal polarizations of incident light. An enhanced SHG signal could be expected at half of the wavelength where EM coupling happens. By extending simulation to SH regime, we show that the intensity of SHG signal could be continuously controlled by rotating the polarization of light source. In addition, we adopt an equivalent circuit model of the designed metamolecule to interpret light manipulation in SH regime with EM coupling by tuning (i) gap size and (ii) refractive index of filling material.

2. Optical Switching On-Off of EM Coupling

Let us begin by briefly explaining the concept of EM coupling in bianisotropic metamolecule. In Maxwell's theory of electromagnetism, the electric field **E** and magnetic field **H** are equivalent when light propagates in free space. However, in natural optical materials this equivalence no longer holds due to weakness of magnetic effect compared with electric component. Surprisingly, optical magnetism has been realized recently through EM coupling, namely bianisotropy, by properly tailoring nanostructures. The underlying mechanism comes from the concept of metamolecule, whereby the optical response can be arbitrarily shaped by engineering the material and morphology of nanostructures.

Herein, let us consider the local electric field $\mathbf{E}^{\mathrm{loc}}$ and magnetic field $\mathbf{H}^{\mathrm{loc}}$ rather than the nonlocal case, concerning that the electromagnetic wave is highly localized down to nanoscale in metamolecules. Besides, we only care about the electric and magnetic dipole moments since higher order multipoles contribute little to the radiation pattern of a bianisotropic metamolecule. With these assumptions, induced electric dipole moment $\mathbf{p}$,

magnetic dipole moment $\mathbf{m}$, and the local field $\left(\mathbf{E}^{\text{inc}}, \mathbf{H}^{\text{inc}}\right)$ are related by following Tellegen formulas:[37]

$$\begin{aligned} \mathbf{p} &= \hat{\alpha}^{\text{ee}}\mathbf{E}^{\text{loc}} + \hat{\alpha}^{\text{em}}\mathbf{H}^{\text{loc}}, \\ \mathbf{m} &= \hat{\alpha}^{\text{mm}}\mathbf{H}^{\text{loc}} + \hat{\alpha}^{\text{me}}\mathbf{E}^{\text{loc}}, \end{aligned} \tag{1}$$

where $\mathbf{E}^{\text{loc}} = \mathbf{E}^{\text{inc}} + \hat{\beta}^{\text{ee}}\mathbf{p}$ and $\mathbf{H}^{\text{loc}} = \mathbf{H}^{\text{inc}} + \hat{\beta}^{\text{mm}}\mathbf{m}$. $\hat{\alpha}^{\text{ee}}, \hat{\alpha}^{\text{mm}}$ and $\hat{\alpha}^{\text{em}}, \hat{\alpha}^{\text{me}}$ are the electric, magnetic and electromagnetic, magnetoelectric polarizability dyadic of metamolecule, respectively. The parameters $\hat{\beta}^{\text{ee}}$ and $\hat{\beta}^{\text{mm}}$ relates the electric dipole moment $\mathbf{p}$ and magnetic dipole moment $\mathbf{m}$ with the local electric and magnetic field, respectively.

After explaining the basic concept of bianisotropy, we move to unveiling EM coupling localized in bianisotropic metamolecules and its potential in SHG manipulation. To this end, we design a metamolecule which consists of four uniform gold nanodisks with radius of 50 nm and thickness of 30 nm, as schematically illustrated in **Figure 1a**. There are two reasons to choose this morphology. First, EM coupling resonance can be more effectively enhanced in a cluster composed of even-numbered particles than in that of odd-numbered particles.[56] Second, nanodisk saves computation memories in comparison with nanosphere. In order to achieve bianisotropy, we firstly put metamolecule into a 2D square pattern with 2nm separation between isolate nanodisks. According to the group theory, EM coupling is not supported in this symmetry metamolecules, where the electric dipole and magnetic dipole modes belong to different symmetry group. [35, 40] Therefore, in our theoretical investigation symmetric-breaking is introduced by shifting the position of two mirrored nanodisks to opposite orientation along x-axis. We did not consider size deviation of nanodisks to introduce symmetry-breaking since it often gives rise to asymmetry in x and y directions simultaneously.

Figure 1b plots the linear scattering cross section (SCS) of the designed asymmetric metamolecule under normal illumination with two orthogonal polarizations. For y-

polarization, only a broad and strong resonance near 745 nm exists, corresponding to electric dipole resonance. In contrast, for x-polarization, a Fano-like dip is obtained near 840 nm, which can be taken as a result of EM coupling in the metamolecule and low radiation losses.

Figure 1c plots the electric and magnetic near-field distributions under both x- and y-polarization at 840 nm (marked by a red arrow in Figure 1b). For x-polarization, the energy is highly localized at the surface of nanodisks, whereas for y-polarization, the energy is much more radiative to far field. That is to say in EM coupling case, a significant part of energy is transferred from electric dipole to magnetic dipole, leading to a large enhancement of electromagnetic field in near-field and suppression of far-field radiation. This feature provides a chance to enhance the SHG signal in comparison with electric resonances.[55]

Overall, Figures 1b and 1c imply the great potential to utilize the designed bianisotropic metamolecule for manipulation of emitted SH signal owing to two key features of EM coupling: (i) highly sensitive to the variation of plasmonic condition and (ii) relatively low radiation. In the following, we will prove this potential.

3. EM coupling and SHG emission

Before describing our study on SHG, we would like to briefly recall SH effect driven by local optical field in metamolecule. As is known, second-order nonlinear processes, such as SHG arising from the nonlinear polarization $\mathbf{P}(2\omega)=\chi^{(2)}:\mathbf{E}(\omega)\mathbf{E}(\omega)$, are forbidden in centrosymmetric materials with the electric dipole approximation of light-matter interaction ($\chi^{(2)}_{\text{bulk}}=0$). In consequence, a lack of centrosymmetry is necessary for allowing the emission of second-order light. The requirement of centrosymmetry breaking can be locally satisfied at the metal surface because of the finite dimension of the atomic lattice, giving rise to surface SHG.[54, 57-60] When the surface anisotropy is neglected, only the $\chi^{(2)}_{\perp\perp\perp}$, $\chi^{(2)}_{\perp\parallel\parallel}$, $\chi^{(2)}_{\parallel\parallel\perp}$, and $\chi^{(2)}_{\parallel\perp\parallel}$ components of the nonlinear susceptibility $\chi^{(2)}$ do not vanish. Here, $\perp$ and $\parallel$ denotes the

normal and tangential component, respectively. Therefore, the relationship between SHG intensity I_{SHG} and the fundamental local electric field $\mathbf{E}^{\mathrm{loc}}(\omega)$ can be approximately given as

$$I_{\mathrm{SHG}} \propto \mathbf{P}(2\omega) = \chi^{(2)}_{\perp\perp\perp} : \mathbf{E}^{\mathrm{loc}}(\omega)\mathbf{E}^{\mathrm{loc}}(\omega) \tag{2}$$

which indicates that efficient SHG signal can be well controlled through the fundamental electric field. It should be noted that the actual SHG to the far field can be different from the SHG generated locally. The actual radiation depends on the plasmonic resonance features in a complex way.[57]

Hereafter, we show that EM coupling in bianisotropic metamolecule could be utilized to manipulate plasmonic SHG signal, including the emitted intensity and frequency. A two-steps full-wave simulation has been performed to calculate the linear and SH scattering progresses, which is described in more detailed in the simulation method part.

As a starting analysis, we compute the dependence of emitted SHG signal from a bianisotropic metamolecule on the polarization angle. As an example, we build a simulation model of metamolecule with $g_1 = 2$ nm and $g_2 = 10$ nm while keep symmetry along y-axis, as illustrated in inset of **Figure 2b**. We continuously rotate the polarization of normal illumination clockwise from y- to x-polarization. Figure 2a plots the simulated SHG as a function of polarization angle and fundamental wavelength. The spectral features of SHG are in good agreement with the analytical prediction above. At fundamental EM coupling wavelength λ=856 nm, SHG efficiency reaches the maximum value and exhibits a narrow peak for x-polarization, then falls continuously to a minimum value (~50 times smaller) for y-polarization. Besides the EM coupling, a relatively weak enhancement is observed at fundamental wavelength λ=588 nm, which can be attributed to low radiative electric quadrupole mode. Figure 2b plots the SHG efficiency which is extracted along the white dashed line in Figure 2a, denoting the switching on-off of SHG with EM coupling. Note that,

due to the intrinsic property of near-field enhancement at plasmonic nanostructure surfaces, the SH emission will not be zero even through the EM coupling shuts down.

With the discussion above in mind, we decide to extend the manipulation of SHG signal. As is known, in addition to optical switching, tailoring frequency is another ancient issue of nonlinear optics.[2] To pursue this goal, metamolecules offer a new avenue due to the intense relation between its optical characteristic and morphology, which can be described by a simplified inductor-capacitor (LC) circuit model.[61] In this model, plasmonic unit cell and the surrounding medium can be effectively treated as nanoinductor and nanocapacitor, respectively. The inductance and capacitance are determined by the geometry parameters and the materials.[62, 63]

As presented in **Figure 3a**, EM coupling results in a circulation of induced current within the designed metamolecule. Thus, in Figure 3b we provide an equivalent circuit model of our designed metamolecule at EM coupling resonance. According to the nanocircuit paradigm, the resonance frequency of EM coupling can be approximately estimated by the relation $\omega_0 = 1/\sqrt{L_{\text{disk}} C_{\text{gap}}}$. Because we break metamolecule symmetry through tuning the gap rather than particle, it means inductance of nanodisk L_{disk} is constant and capacitance of gap $C_{\text{gap}} \propto \varepsilon_0 \varepsilon_{\text{d}} S/g$ varies with permittivity of filling material and the gap size g , where S is the effective area of capacitive gap. Hence in the following parts we will investigate the manipulation of emitted SHG frequency with the EM coupling from two aspects: (i) gap size g_2 and (ii) filling material index.

First, in order to explore the effect of the gap size on emitted SHG signal, we compare both linear and SH optical responses of five structures with $g_1 = 2$ nm, $g_2 = 2$ nm, 6 nm, 10 nm, 14 nm and 18 nm.

Figure 4a and 4b shows the simulated linear SCS and SHG efficiency, respectively, of these metamolecules under normal incidence with x- and y-polarization. When $g_2 = 2$ nm, the linear SCSs of metamolecule exhibit totally same feature and only the electric dipole resonance is excited by the incident plane wave, since the structure is symmetric and equivalent along x- and y-axis. In these symmetric cases, EM coupling cannot be opened up under the normal incidence and electric dipole resonance dominates in scattering, thereby leading to high radiation to far field rather than localization at the surface of metamolecule. In consequence, their SHG signals are only slightly enhanced at electric quadrupole resonance. In contrast, when $g =$ 6 nm, 10 nm, 14 nm and 18 nm, the metamolecules are asymmetric and symmetric along x- and y-axis, respectively. For y-polarization, both the linear SCS and SHG efficiency show little variation in comparison with that of symmetric metamolecule, indicating that no EM coupling happens. For x-polarization, a Fano-like dip, induced by EM coupling, appears around wavelength of 850 nm in the linear SCS spectra. Correspondingly, the emitted SHG signal from metamolecule is enhanced at half of the EM coupling wavelength attributing to low radiation loss.

These simulation results are in qualitatively agreement with the LC circuit model predictions that the enhanced SHG efficiency gradually shifts to the high energies when the gap size g_2 increases, as indicated by a black dotted line in Figure 4b. By increasing g_2, the capacitance of the gap $C_{\text{gap}} \propto \varepsilon_0 \varepsilon_{\text{d}} S/g$ reduces, resulting in weak capacitive coupling and light-matter interaction within metamolecule. Hence the eigen-frequency $\omega_0 = 1/\sqrt{L_{\text{disk}} C_{\text{gap}}}$ of EM coupling resonance and corresponding enhanced SHG signal will blue shifts. Besides, Figure 4a also shows mode splitting of electric dipole resonance under x-polarization due to the gap size $g_1 \neq g_2$.

In order to understand the underlying physical mechanism, we additionally calculated near-field distributions and far-field patterns, as shown in **Figure 5**. As an example, we choose points A, B, and C as marked in Figure 4a. For x-polarization, the near-field intensity will be enhanced at all points A, B, and C as shown in Figure 5a. At points A and B, electric field prefers to concentrate in gap g_1 and g_2, respectively, revealing the splitting of electric dipole resonances. At point C, electric field forms a close loop within metamolecule, thereby leading to strong EM coupling and low radiation. Figure 4b shows corresponding magnetic field distributions. In contrast to points A and B, at point C magnetic field is enhanced significantly at centre of metamolecule, demonstrating the clear characteristic of EM coupling. For comparison, we also calculated the y-polarization cases, as plotted in Figures 4e and 4f. These results show that the electromagnetic fields are localized within the gaps along y-axis, consistent with the highly radiation of electric dipole resonance. Unsurprisingly, both the near-field and far-field intensities of emitted SH signal for the EM coupling resonance is much stronger than that for the electric dipole resonances, as can be seen in Figures 4c, 4g and 4d, 4h.

Second, we concentrate on the active manipulation of emitted SH signal with EM coupling by changing the filling material between the isolate nanodisks. To this end, we use normal illumination with x-polarization. The gap sizes are $g_1 = 2$ nm and $g_2 = 10$ nm. As examples, we perform simulations for cases of filling dielectric material $n = 1.0$, 1.1, 1.2, 1.3.

Figure 6 plots the SHG efficiency normalized to the maximum of $n = 1.0$ case as a function of filling dielectric material at fundamental wavelength. As expected, higher refractive index of dielectric possesses more free electrons within the gaps of metamolecule, thus the capacitive coupling between each isolate nanodisk becomes stronger. Correspondingly, the electromagnetic coupling mode progressively stores more energy at the surface of nanostructure, accompanied with red-shift of EM coupling resonance. In other words, the high

density of the surrounding medium allows a strong nonlinear interaction with incoming electromagnetic field that occupies the nanoscale volume. In consequently, the emitted SH efficiency will be enhanced and SH can generate light source with longer wavelength, which is in agreement with the LC circuit model.

The dependence of emitted SH signal on filling material is a manifestation of that we could active manipulate SH signal, thereby paving the way for a deeper understanding of the nonlinear action of light with plasmonic nanostructure and, eventually, for the design of future practical applications. For examples, there are two increasing popular techniques which could be applied in active controlling of emitted SH signal: (i) applying voltage to modify the carrier concentration[64] and (ii) temperature-dependent change of filling dielectric.[65-67]

4. Conclusion

In summary, electromagnetic coupling in a bianisotropic metamoleclue has been utilized to control light in SH regime, including switching on-off and generating different frequency. The electromagnetic coupling results in high near-field intensity and low radiation, which could be beneficial to SHG. Thus, the switching of electromagnetic coupling with polarization angle allows us to continuously tune the SHG efficiency. Furthermore, according to an equivalent LC circuit model, the frequency of generating SH source has been well manipulated by adjusting the geometry and materials of the gaps. Our results show the potential of bianisotropic metamolecules for controlling light in both linear and nonlinear regimes, paving the way to application in optoelectronic devices.

5. Simulation Methods of Linear and SH Cases

FEM simulations were performed to calculate the linear and nonlinear optical response of the proposed nanostructure by using the commercial software COMSOL Multiphysics. The optical constant of gold was taken from Johnson and Christy's work.[68] For simplicity, the refractive index of surrounding dielectric material is set to be non-dispersive. Mesh size of

1~3 nm and 5~10 nm were utilized in the gap of gold nanodisks and the rest of calculation space, respectively, to ensure accuracy and save computation time simultaneously.

A two-steps simulation has been adopted. First, a total-field-scattering background source was employed to remove the incident light from scattering signals. We could obtain the near-field distribution for the linear case. Second, an effective nonlinear current sheet at the surface of nanostructure has been applied as the source of second harmonic scattering process with the use of weak form. Then, both the near-field and far-field distributions can be computed with scattering model at SH frequency. In our case, only the dominant component $\chi_{\perp\perp\perp}$ of the second order surface susceptibility tensor was considered, where $\perp$ represents the orientation perpendicular to the surface of the structure. Note that, there are some other theoretically allowed but negligible contributions to SH signal.

Acknowledgements

We acknowledge financial support from Hong Kong Research Grant Council (AoE/P-02/12) and Hong Kong Polytechnic University (1-ZVGH).

Conflict of Interest

The authors declare no conflict of interest.

Received: ((will be filled in by the editorial staff))
Revised: ((will be filled in by the editorial staff))
Published online: ((will be filled in by the editorial staff))

References

[1] Born, M.; Wolf, E. *Principles of Optics: Electromagnetic Theory of Propagation Interference and Diffraction of Light*; Sixth Edition; Pergamon Press, **1980**.

[2] Boyd, R. W. *Nonlinear Optics*; Academic Press, **2003**.

[3] Chen, H.; Chan, C. T.; Sheng, P. *Nat. Mater.* **2010**, 9, 387-396.

[4] Meinzer, N.; Barnes, W. L.; Hooper, I. R. *Nat. Photon.* **2014**, 8, 889-898.

[5] Shelby, R. A.; Smith, D. R.; Schultz, S. *Science* **2001**, 292, 77-79.

[6] Fan, X.; Wang, G. P.; Lee, J. C. W.; Chan, C. T. *Phys. Rev. Lett.* **2006**, 97, 073901.

[7] Valentine, J.; Zhang, S.; Zentgraf, T.; Ulin-Avila, E.; Genov, D. A.; Bartal, G.; Zhang, X. *Nature* **2008**, 455, 376-379.

[8] Silveirinha, M.; Engheta, N. *Phys. Rev. Lett.* **2006**, 97, 157403.

[9] Hao, J.; Yan, W.; Qiu, M. *Appl. Phys. Lett.* **2010**, 96, 101109.

[10] Vesseur, E.; Coenen, T.; Caglayan, H.; Engheta, N.; Polman, A. *Phys. Rev. Lett.* **2013**, 110, 013902.

[11] Shin, J.; Shen, J. T.; Fan, S. *Phys. Rev. Lett.* **2009**, 102, 093903.

[12] Hao, J.; Yuan, Y.; Ran, Li.; Jiang, T.; Kong, J. A.; Chan, C. T.; Zhou, Lei. *Phys. Rev. Lett.* **2007**, 99, 063908.

[13] Cui, Y.; Fung, K. H.; Xu, J.; Ma, H.; Jin, Y.; He, S.; Fang, N. X. *Nano Lett.* **2012**, 12, 1443-1447.

[14] Guo, K.; Liu, J.; Zhang, Y.; Liu, S. *Opt. Express* **2012**, 20, 28586-28593.

[15] Campione, S.; Guclu, C., Ragan, R.; Capolino, F. *ACS Photonics* **2014**, 1, 254-260.

[16] Bao, Y.; Hu, Z.; Li, Z.; Zhu, X.; Fang, Z. *Small* **2015**, 11, 2177-2181.

[17] Monticone, F.; Alu, A. *J. Mater. Chem. C* **2014**, 2, 9059.

[18] Ponsinet, V.; Barois, P.; Gali, S. M.; Richetti, P.; Salmon, J. B.; Vallecchi, A.; Albani, M.; Le Beulze, A.; Gomez-Grana, S.; Duguet, E.; Mornet, S.; Treguer-Delapierre, M. *Phys. Rev. B* **2015**, 92, 220414(R).

[19] Qin, L.; Zhang, K.; Peng, R. W.; Xiong, X.; Zhang, W.; Huang, X. R.; Wang, M. *Phys. Rev. B* **2013**, 87, 125136.

[20] Markovich, D.; Baryshnikova, K.; Shalin, A.; Samusev, A.; Krasnok, A.; Belov, P.; Ginzburg, P. *Sci. Rep.* **2016**, 6, 22546.

[21] Lapine, M.; Shadrivov, I. V.; Kivshar, Y. S. *Rev. Mod. Phys.* **2014**, 86, 1093-1123.

[22] Rahmani, M.; Shorokhov, A. S.; Hopkins, B.; Miroshnichenko, A. E.; Shcherbakov, M. R.; Camacho-Morales, R.; Fedyanin, A. A.; Neshev, D. N.; Kivshar, Y. S. *ACS Photonics* **2017**, 4, 454-461.

[23] Makarov, S. V.; Petrov, M. I.; Zywietz, U.; Milichko, V.; Zuev, D.; Lopanitsyna, N.; Kuksin, A.; Mukhin, I.; Zograf, G.; Ubyivovk, E.; Smirnova, D. A.; Starikov, S.; Chichkov, B. N.; Kivshar, Y. S. *Nano Lett.* **2017**, 17, 3047-3053.

[24] Kruk, S. S.; Camacho-Morales, R.; Xu, L.; Rahmani, M.; Smirnova, D. A.; Wang, L.; Tan, H. H.; Jagadish, C.; Neshev, D. N.; Kivshar, Y. S. *Nano Lett.* **2017**, 17, 3914-3918.

[25] Yang, X.; Zhang, C.; Wan, M.; Chen, Z.; Wang, Z. *Opt. Lett.* **2016**, 41, 2938-2941.

[26] Nookala, N.; Lee, J.; Tymchenko, M.; Gomez-Diaz, J. S.; Demmerle, F.; Boehm, G.; Lai, K.; Shvets, G.; Amann, M. C.; Alu, A.; Belkin, M. *Optica* **2016**, 3, 283-288.

[27] Zhang , Y.; Wen, F.; Zhen, Y. R.; Nordlander, P.; Halas, N. J. *PNAS* **2013**, 110, 9215-9219.

[28] Klein, M. W.; Enkrich, C.; Wegener, M.; Soukoulis, C. M.; Linden, S. *Opt. Lett.* **2006**, 31, 1259-1261.

[29] Hein, S. M.; Giessen, H. *Phys. Rev. Lett.* **2013**, 111, 026803.

[30] Zhang, Q.; Wen, X.; Li, G.;Ruan, Q.; Wang, J.; Xiong, Q. *ACS Nano* **2013**, 7, 11071-11078.

[31] Shafiei, F.; Monticone, F.; Le, K. Q.; Liu, X. X.; Hartsfield, T.; Alu, A.; Li, X. *Nat. Nanotech.* **2013**, 8, 95-99.

[32] Sheikholeslami, S. N.; Aleaian, H.; Koh, A. L.; Dionne, J. A. *Nano Lett*. **2013**, 13, 4137-4141.

[33] Sheikholeslami, S. N.; Garcia-Etxarri A.; Dionne, J. A. *Nano Lett.* **2011**, 11, 3927-3934.

[34] Wang, B.; Zhang Y. *IEEE J. Quantum Elect.* **2015**, 51, 7300108.

[35] Sun, L.; Ma, T.; Yang, S. C.; Kim. D. K.; Lee, G.; Shi, J.; Martinez, I.; Yi, G. R.; Shvets, G.; Li, X. *Nano Lett.* **2016**, 16, 4322-4328.

[36] Verre, R.; Yang, Z. J.; Shegai, T.; Kall, M. *Nano Lett.* **2015**, 15, 1952-1958.

[37] Alaee, R.; Albooyeh, M.; Yazdi, M.; Komjani, N.; Simovski, C.; Lederer, F.; Rockstuhl, C. *Phys. Rev. B* **2015**, 91, 115119.

[38] Kraft, M.; Braun, A.; Luo, Y.; Maier, S. A.; Pendry, J. B. *ACS Photonics* **2016**, 3, 764-769.

[39] Zhang, C.; Fang, J.; Yang, W.; Song, Q.; Xiao, S. *Adv. Opt. Mater.* **2017**, 1700469.

[40] Urzhumov, Y. A.; Shvets G.; Fan, J.; Capasso, F.; Brandl, D.; Nordlander, P. *Opt. Express* **2007**, 15, 14129-14145.

[41] Fung, K. H.; Chan C. T. *Opt. Lett.* **2007**, 32, 973-975.

[42] Fung, K. H.; Chan C. T. *Phys. Rev. B* **2008**, 77, 205423.

[43] Fan, S.; Suh, W.; Joannopoulos, J. D. *J. Opt. Soc. Am. A* **2003**, 20, 569-572.

[44] Liu, N.; Mukherjee, S.; Bao, K.; Li, Y.; Brown, L. V.; Nordlander, P.; Halas, N. J. *ACS Nano* **2012**, 6, 5482-5488.

[45] Xiong, X.; Sun, W. H.; Bao, Y. J.; Peng, R. W.; Wang, M.; Sun, C.; Lu, X.; Shao, J.; Li, Z. F.; Ming, N. B. *Phys. Rev. B* **2009**, 80, 201105(R).

[46] Pferffer, C.; Zhang, C.; Ray, V.; Guo, L. J.; Grbic, A. *Phys. Rev. Lett.* **2014**, 113, 023902.

[47] Yazdi, M.; Albooyeh, M.; Alaee, R.; Asadchy, V.; Komjani, N.; Rockstuhl, C.; Simovski, C. R.; Tretyakov, S. *IEEE T. Antenn. Propag.* **2015**, 63, 3004-3015.

[48] Yang, Z. J.; Hao, Z. H.; Lin, H. Q.; Wang, Q. Q. *Nanoscale* **2014**, 6, 4985-4997.

[49] Wang, J.; Fan, C.; He, J.; Ding, P.; Liang, E.; Xue, Q. *Opt. Express* **2013**, 21, 2236-2244.

[50] Klein, M. W.; Enkrich, C.; Wegener, M.; Linden, S. *Science* **2006**, 313,502-504.

[51] Miroshnichenko, A. E.; Flach, S.; Kivshar, Y. S. *Rev. Mod. Phys.* **2010**, 82, 2257-2298.

[52] Zhang, S.; Li, G. C.; Chen, Y.; Zhu, X.; Liu, S. D.; Lei, D. Y.; Duan, H. *ACS Nano* **2016**, 10, 11105-11114.

[53] Wen, Y.; Zhou, J. *Phys. Rev. Lett.* **2017**, 118, 167401.

[54] Ciraci, C.; Poutrina, E.; Scalora, M.; Smith, D. R. *Phys. Rev. B* **2012**, 86, 115451.

[55] Yang, D. J.; Im, S. J.; Pan, G. M.; Ding, S. J.; Yang, Z. J.; Hao, Z. H.; Wang, Q. Q. *Nanoscale* **2017**, 9, 6068-6075.

[56] Alu, A.; Engheta, N. *Phys. Rev. B* **2008**, 78, 085112.

[57] Butet, J.; Brevet, P. F.; Martin, O. J. F. *ACS Nano* **2015**, 9, 10545-10562.

[58] Thyagarajan, K.; Butet, J.; Martin, O. J. F. *Nano Lett.* **2013**, 13, 1847-1851.

[59] Walsh, G. F.; Negro, L. D. *Nano Lett.* **2013**, 13, 3111-3117.

[60] Xiong, X. Y. Z.; Al-Jarro, A.; Jiang L. J.; Panoiu, N. C.; Sha, W. E. I. *Phys. Rev. B* **2017**, 95, 165432.

[61] Engheta, N.; Salandrino, A.; Alu, A. *Phys. Rev. Lett.* **2005**, 95, 095504.

[62] Liu, N.; Wen, F.; Zhao, Y.; Wang, Y.; Nordlander, P.; Halas, N. J.; Alu, A. *Nano Lett.* **2013**, 13, 142-147.

[63] Feng, R.; Qiu, J.; Liu, L.; Ding, W.; Chen, L. *Opt. Express* **2014**, 22, A1713-A1724.

[64] Yan, J.; Ma, C.; Liu, P.; Wang, C.; Yang, G. *Nano Lett.* **2017**, 17(8), 4793-4800.

[65] Rahmani, M.; Xu, L.; Miroshnichenko, A. E.; Komar, A.; Camacho-Morales, R.; Chen, H.; Zarate, Y.; Kruk, S.; Zhang, G.; Neshev, D. N.; Kivshar, Y. *Adv. Funct. Mater.* **2017**, 1700580.

[66] Zhu, W.; Rukhlenko, I. D.; Xiao, F.; He, C.; Geng, J.; Liang, X.; Premaratne, M.; Jin, R. *Opt. Express* **2017**, 25, 15737-15745.

[67] Hu, J.; Lang, T.; Shi, G. H. *Opt. Express* **2017**, 25, 15241-15251.

[68] Johnson, P. B.; Christy, R. W. *Phys. Rev. B* **1972**, 6, 4370.

((Insert Figure here. Note: Please do not combine figure and caption in a textbox or frame.))

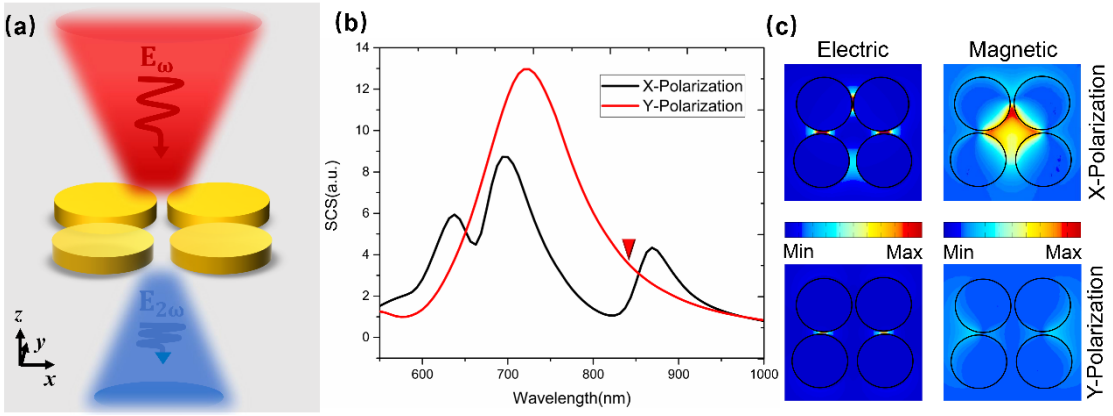

Figure 1. (a) Schematic of bianisotropic metamolecule in which the electromagnetic coupling could happen. The four gold nanodisks with radius of $r = 50\,\text{nm}$ and thickness of $t = 30\,\text{nm}$, are symmetric and asymmetric along y-axis and x-axis, repectively. Light is incident from the top of metamolecule with electric field polarizing along x- or y-axis. (b) Linear scattering cross section (SCS) of the metamolecule at fundamental frequency under normal incident light with x- (black line) and y- (red line) polarization. The red arrow denotes the wavelength of the electromagnetic coupling under x-polarization. (c) Normalized electric and magnetic near-field distributions at the fundamental wavelength denoted by red arrow in (b). Top panels: x-polarization. Bottom panels: y-polarization.

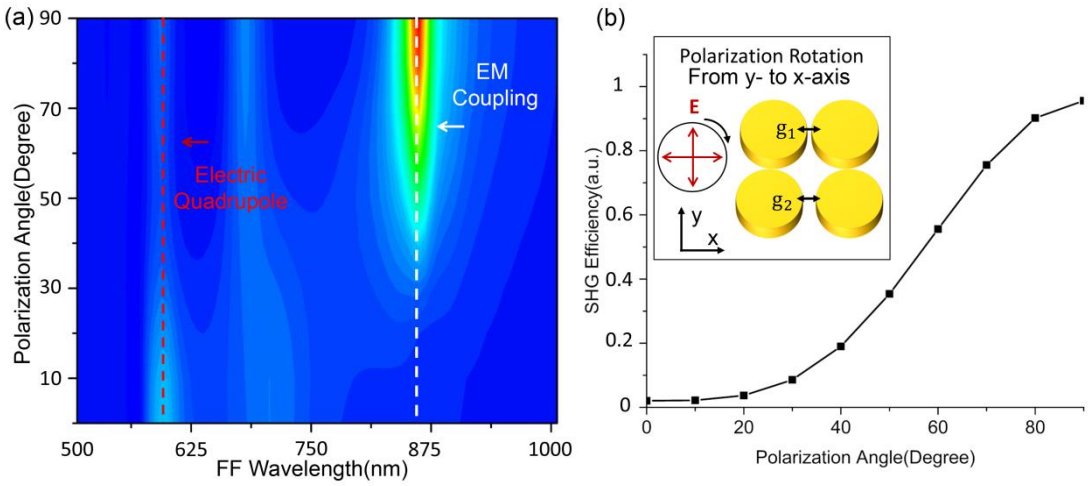

Figure 2. (a) Polarization dependent SHG efficiency spectra of the designed bianisotropic metamolecule. The white and red dashed line marks the wavelength of electromagnetic coupling and electric quadrupole at the fundamental frequency wavelength, respectively. (b) The dependence of SHG efficiency on polarization of the incident light at the fundamental magnetic resonance (EM coupling). Inset: illustration of the polarization rotation.

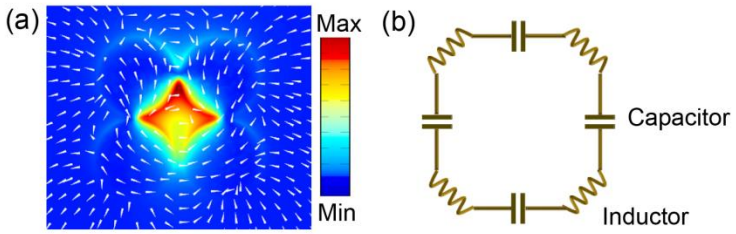

Figure. 3 (a) Near-field profiles of magnetic field and induced current at the EM coupling wavelength. (b) Corresponding equivalent circuit evolution, showing that the designed metamolecule can be interpreted as a close-loop of LC circuit.

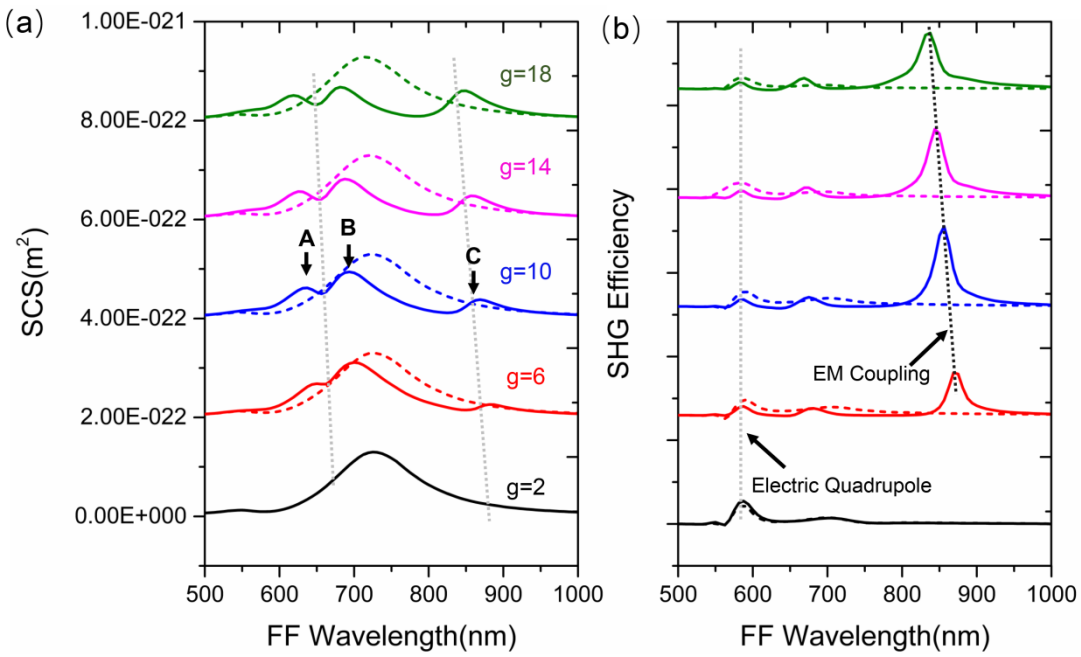

Figure 4. Active controlling of the electromagnetic coupling and emitted SHG efficiency with the gap size g_2 between the bottom two particles under x- (solid line) and y-polarized (dashed line) light. (a) The scattering cross section and (b) the SHG efficiency of the metamaterial with radius of 50 nm, thickness of 30 nm, and gap size between the bottom two particles of 2 nm, 6 nm, 10 nm, 14 nm and 18 nm.

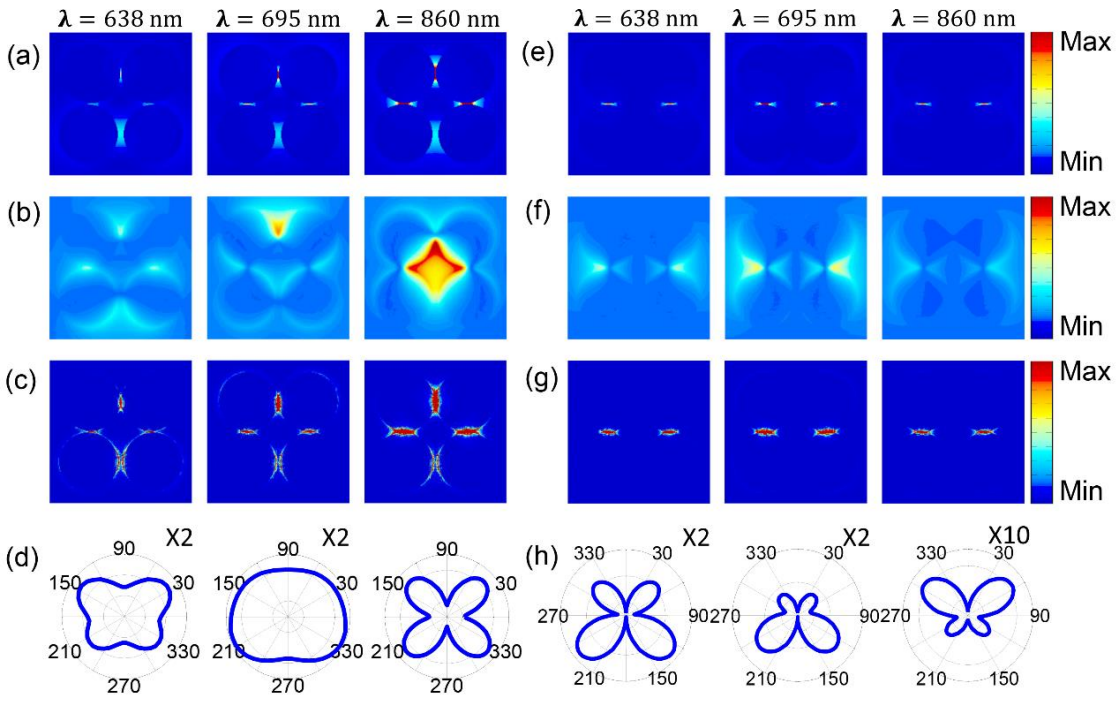

Figure 5. Comparison of the linear and SH responses between the electromagnetic coupling 'on' and 'off'. The simulated near- and far-field distribution of metamaterial under x- (left column) and y-polarized (right column) light at wavelength of 638 nm, 695 nm and 860 nm, which were marked by A, B, C in Fig. 3. The near field distributions of normalized (a, e) electric and (b, f) magnetic field at fundamental frequency, and of (c, g) electric field at SH frequency. The far field distribution of electric field (in **E-k** plane) at SH frequency under (d) x- and (h) y-polarized light.

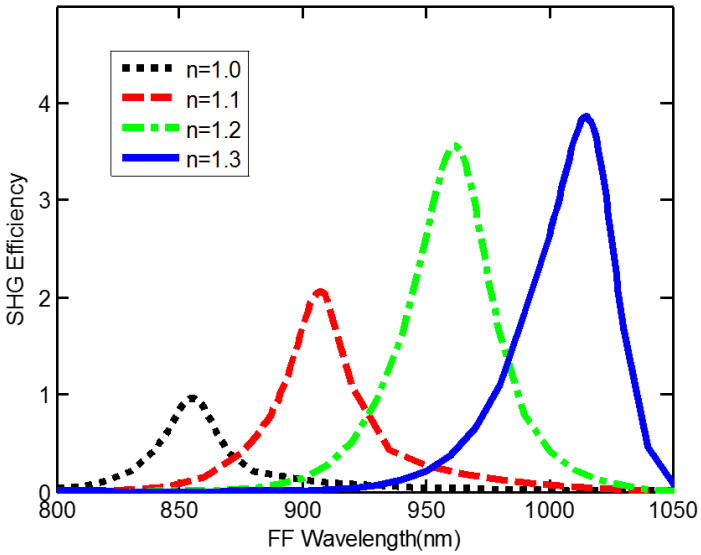

Figure 6. The SHG efficiency as a function of the refractive index of the filling materials within the gaps of bianisotropic metamolecle under x-polarization incidence.

Bianisotropic metamolecules provide a novel opportunity to realize optical magnetism through localized electromagnetic coupling. Here, we investigate the manipulation of second-harmonic generation from a bianisotropic metamolecule, which is composed of four uniform gold nanodisks. Simulation results show that a Fano-like resonance induced by electromagnetic coupling is sufficient to control second harmonic generation signal.

Keyword

plasmonics, nonlinear optics, bianisotropy, metamolecule

Authors

K. Guo, C. Qian, Y. L. Zhang, and K. H. Fung*

Second harmonic generation manipulation enabled by electromagnetic coupling in bianisotropic metamolecules

ToC figure

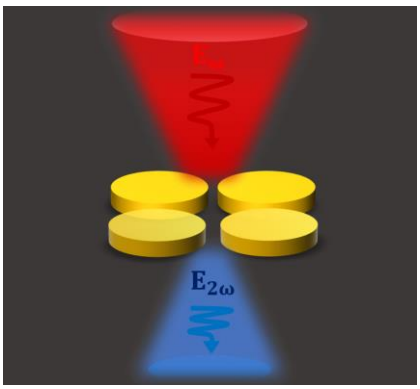

((Supporting Information can be included here using this template))

Supporting Information

Title ((no stars))

*Author(s), and Corresponding Author(s)** ((write out full first and last names))

((Please insert your Supporting Information text/figures here. Please note: Supporting Display items, should be referred to as Figure S1, Equation S2, etc., in the main text…)